Graphene-based glucose sensors with an attomolar limit of detection

Vicente Lopes[1,‡], *Tiago Abreu*[1,2,‡], *Mafalda Abrantes*[1,2], *Siva Sankar Nemala*[1], *Francesco De Boni*[3], *Mirko Prato*[3], *Pedro Alpuim*[1,2,*], *Andrea Capasso*[1,*]

[1] International Iberian Nanotechnology Laboratory, 4715-330 Braga, Portugal

[2] Center of Physics of the Universities of Minho and Porto, University of Minho, 4710-057 Braga, Portugal

[3] Materials Characterization Facility, Istituto Italiano di Tecnologia, Via Morego 30, 16163 Genova, Italy

SUPPLEMENTARY INFORMATION

[*] **Corresponding Authors:** andrea.capasso@inl.int (Andrea Capasso), pedro.alpuim.us@inl.int (Pedro Alpuim)

‡These authors contributed equally.

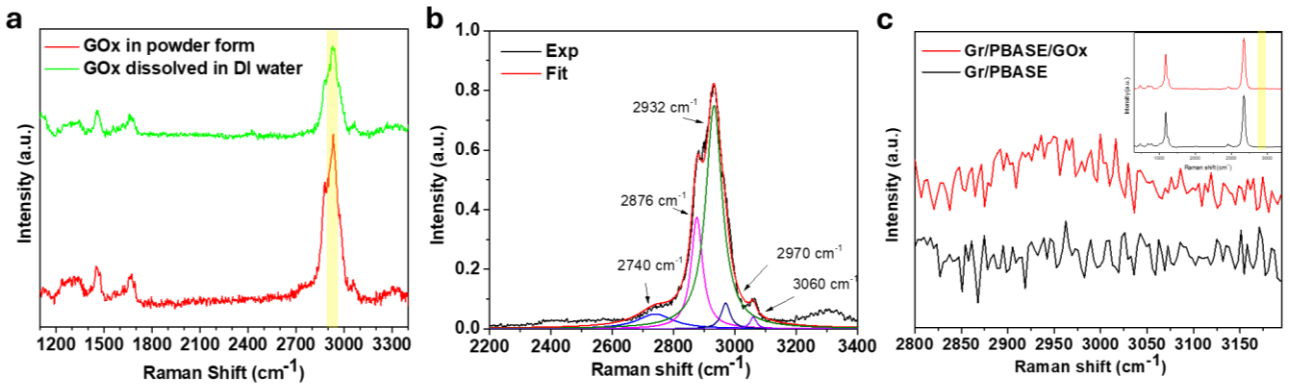

Figure S1. (a) Raman spectra of GOx: powder form and dissolved in DI water. (b) The 2800-3100 cm^{-1} range (highlighted by a yellow stripe in (a)) fitted with Lorentzian functions. (c) Gr/PBASE and Gr/PBASE/GOx spectra zoomed-in in the 2800-3100 cm^{-1} range, showing a small contribution at 2947 cm^{-1} in the Gr/PBASE/GOx spectrum, not visible in Gr/PBASE.

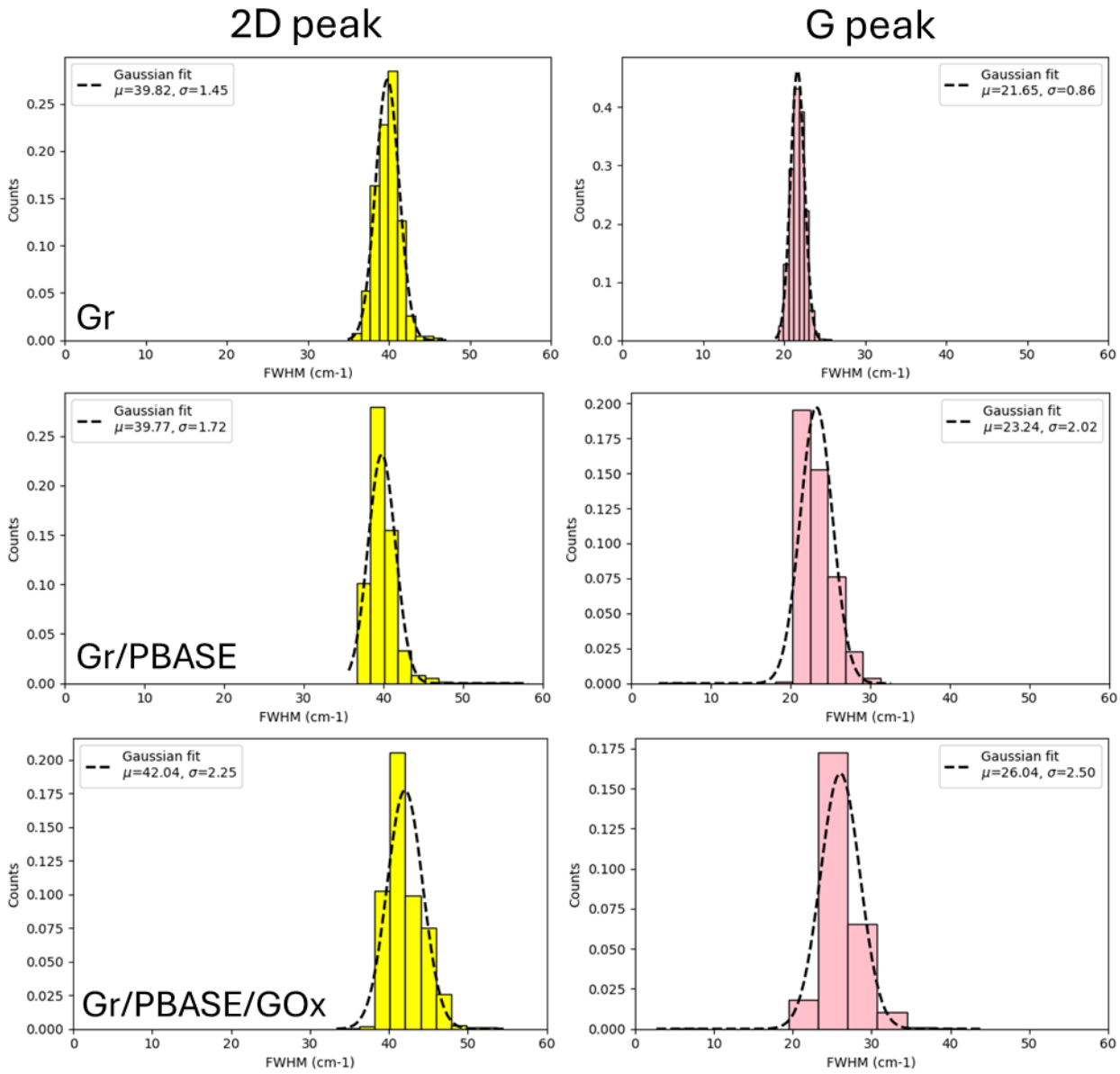

Figure S2. FWHM distribution of the 2D and G peaks of graphene for Gr, Gr/PBASE and Gr/PBASE/GOx.

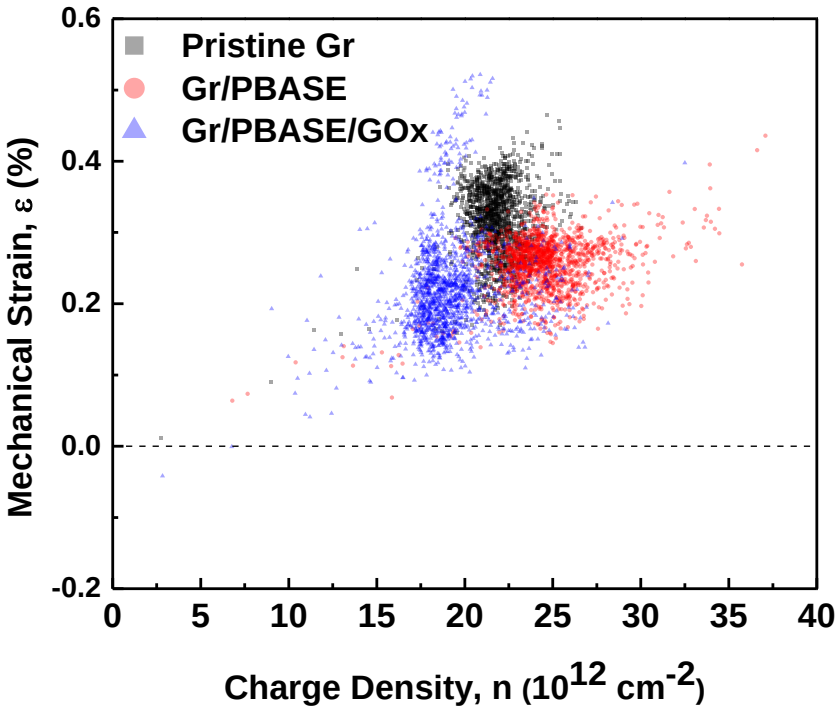

Figure S3. Mechanical strain (ε, %) vs charge (hole) density (n, 10^{12} cm^{-2}) plot of 1500 Raman measurements for each functionalization step. The plot is a linear transformation of the 2D vs G frequency plot shown in Figure 1c.

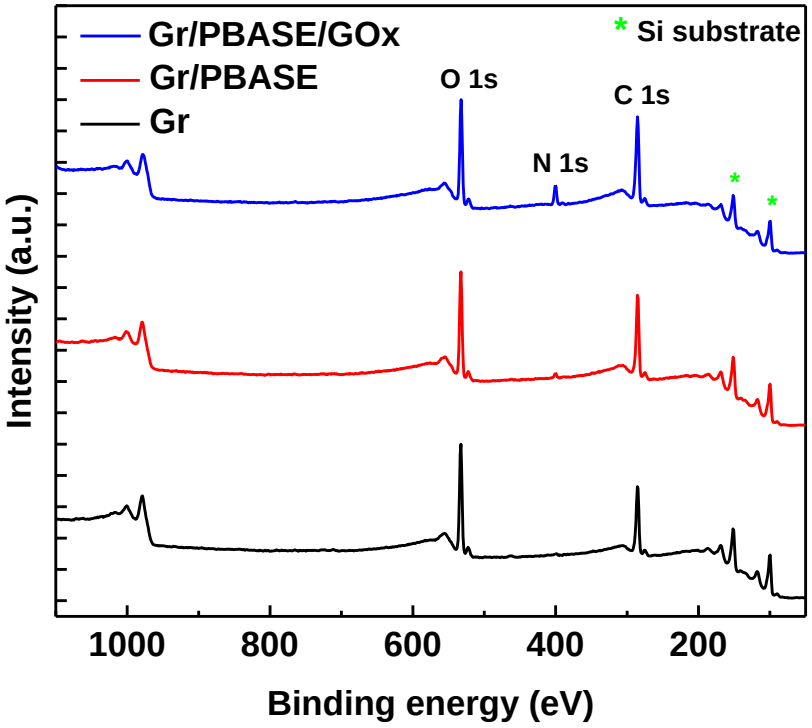

Figure S4. XPS survey spectra for Gr, Gr/PBASE and Gr/PBASE/GOx.

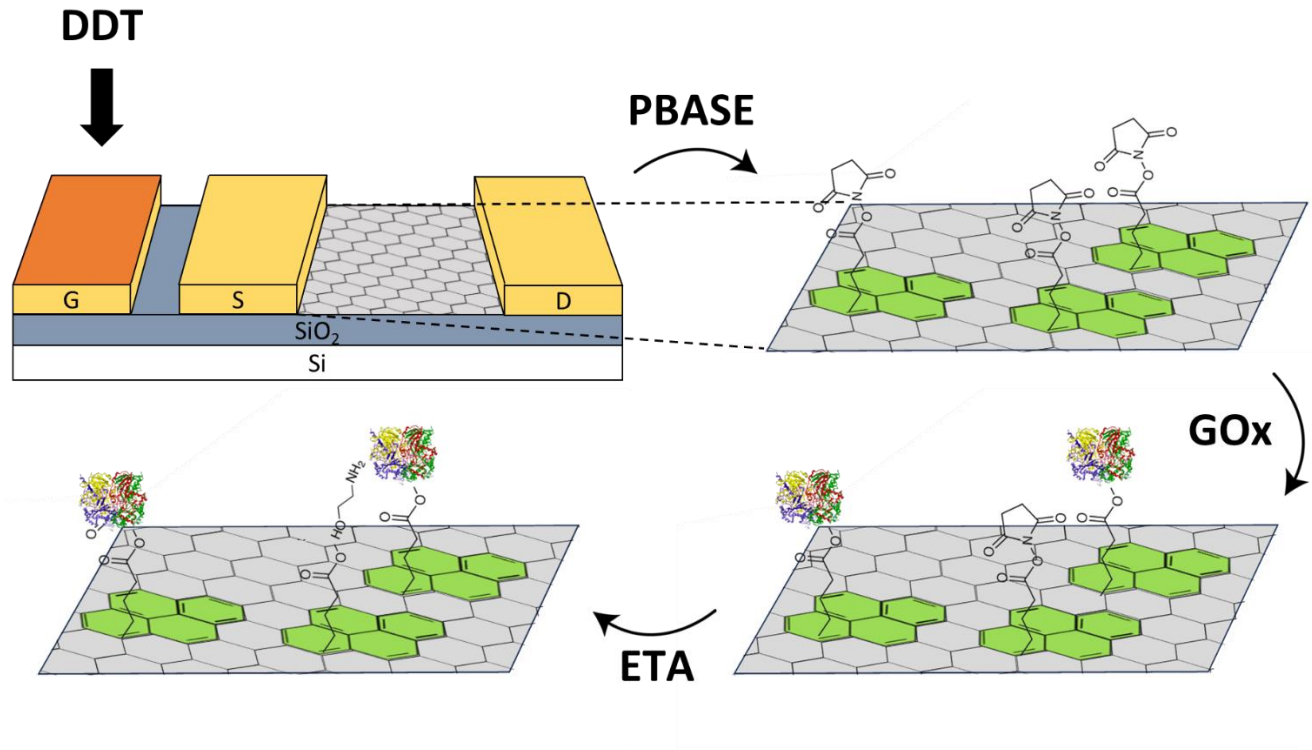

Figure S5. Schematic of the full functionalization process of the EG-GFETs for glucose detection: 1) DDT - Au gate passivation. 2) PBASE - noncovalent modification with pyrene linkers followed by GOx - immobilization of the biorecognition element, GOx. 3) ETA - blocking of unreacted sites of PBASE.

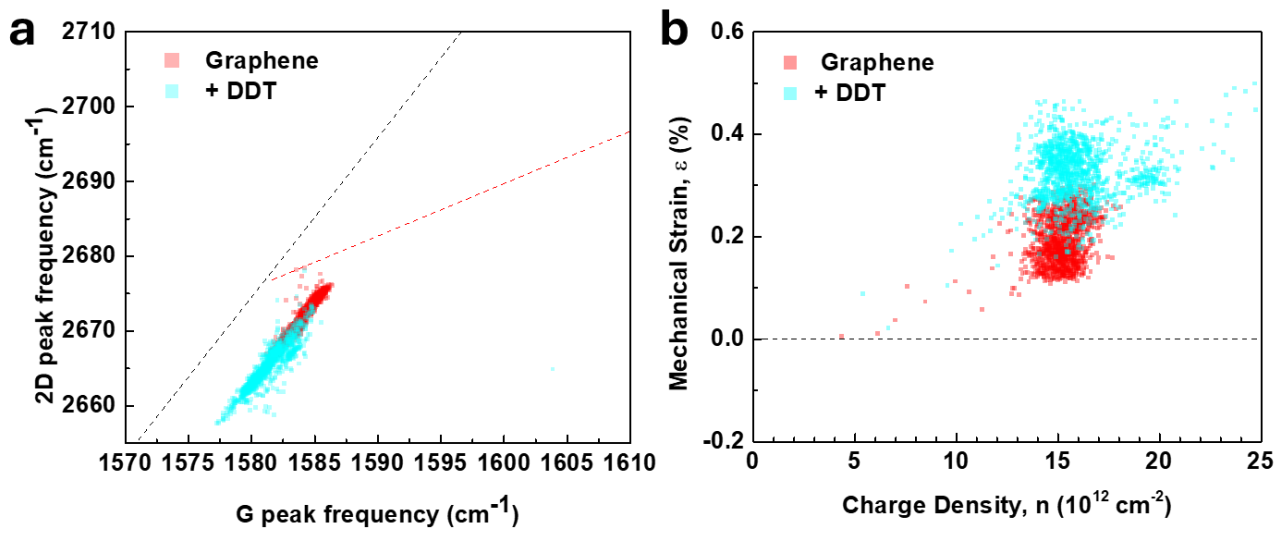

Figure S6. Variation of 2D and G modes frequency after Au passivation with DDT molecules. Visualization on (a) 2D vs G frequency plot and on (b) mechanical strain vs charge density plot. Data are 1500 measurements for each step. In (a), the red dashed line is an average of (ω_G, ω_{2D}) for strain-free graphene with varying density of holes (n, whereas the black dashed line represents a prediction of (ω_G,ω_{2D}) for charge-neutral graphene under randomly oriented uniaxial stress.

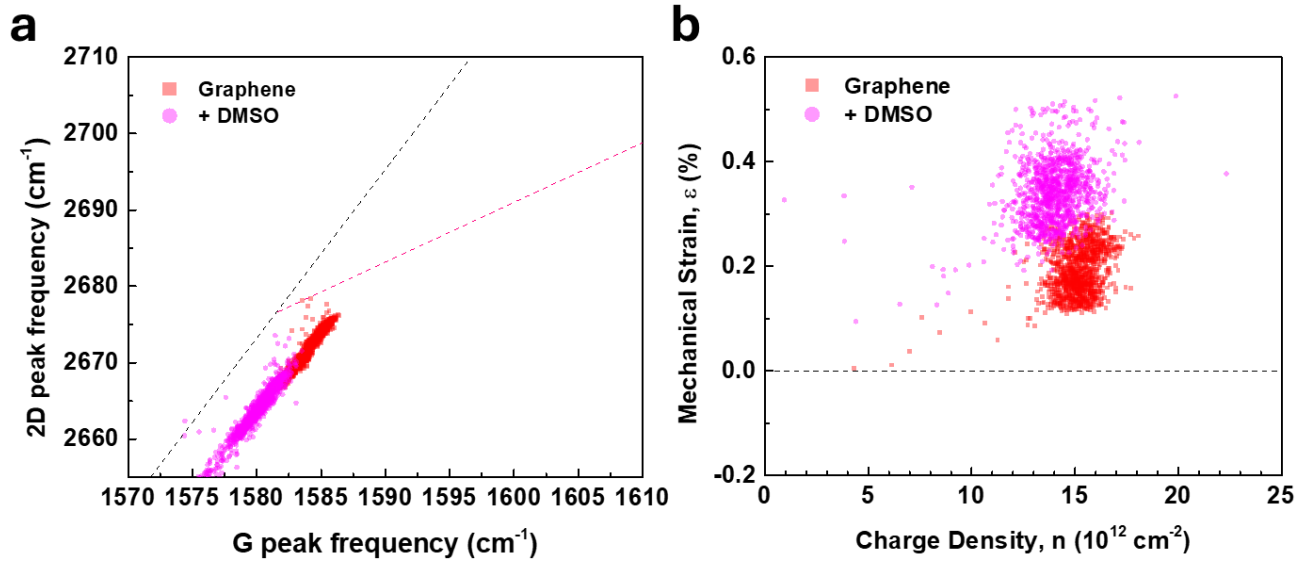

Figure S7. Variation of 2D and G modes frequency after Au passivation with DMSO molecules. Visualization on (a) 2D vs G frequency plot and on (b) mechanical strain vs charge density plot. Data are 1500 measurements for each step. In (a), the red dashed line is an average of (ω_G, ω_{2D}) for strain-free graphene with varying density of holes (n, whereas the black dashed line represents a prediction of (ω_G,ω_{2D}) for charge-neutral graphene under randomly oriented uniaxial stress.

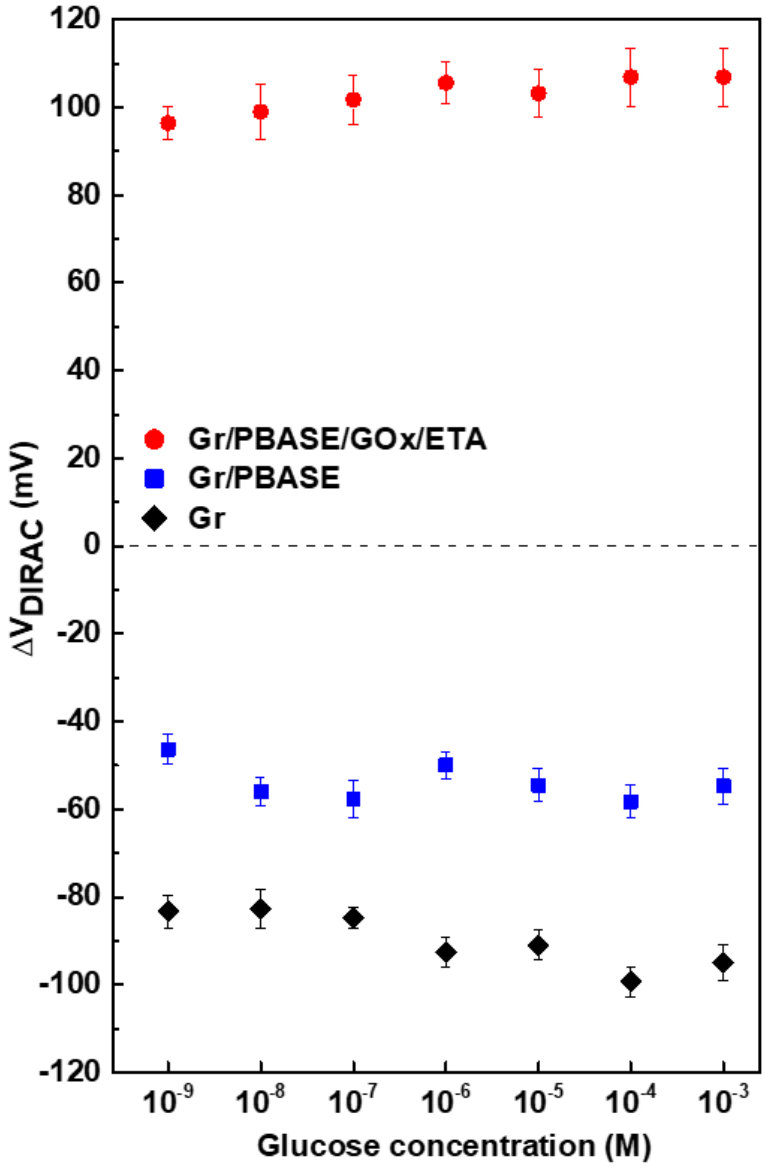

Figure S8. Calibration curves for Gr, Gr/PBASE and Gr/PBASE/GOx/ETA in nM-mM (saturation) range. The three cases show almost no variation with an increase in the glucose concentration.*

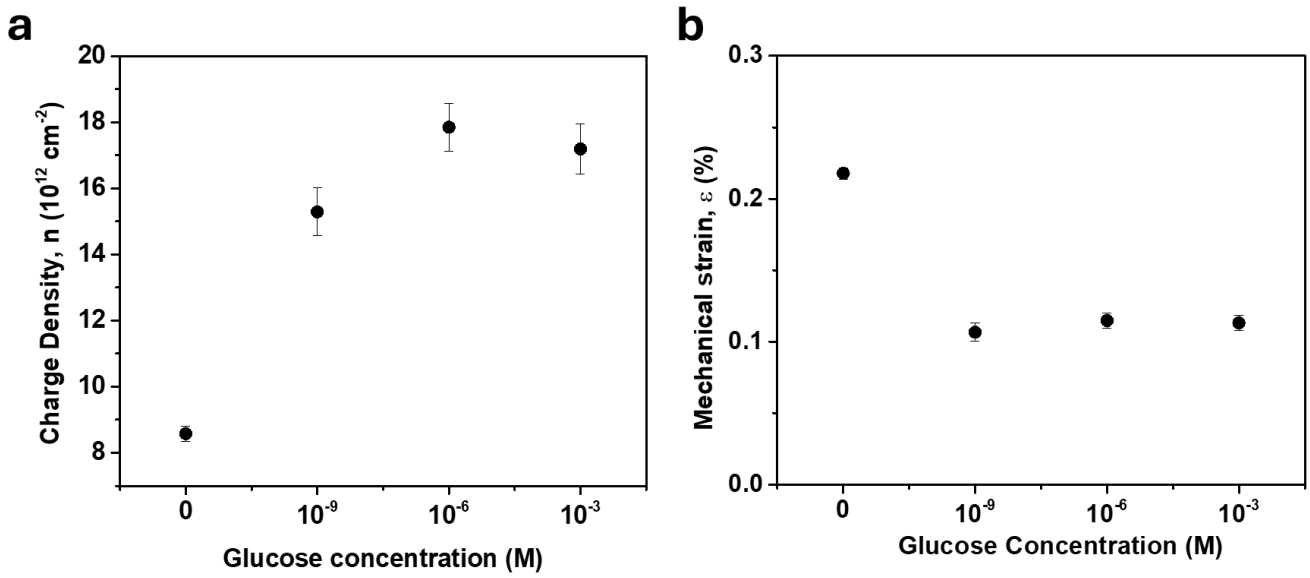

Figure S9. Corresponding (a) charge density and (b) mechanical strain calibration curves extracted from 2D and G position values of Figure 3c. At 1 mM, there is an overall increase in hole concentration of ~ 9 x 10^{12} cm^{-2}. The mechanical strain varies minimally between concentrations (1 nM-1 mM, with a ~ 0.1% increase in compressive strain only after 1 nM was detected.

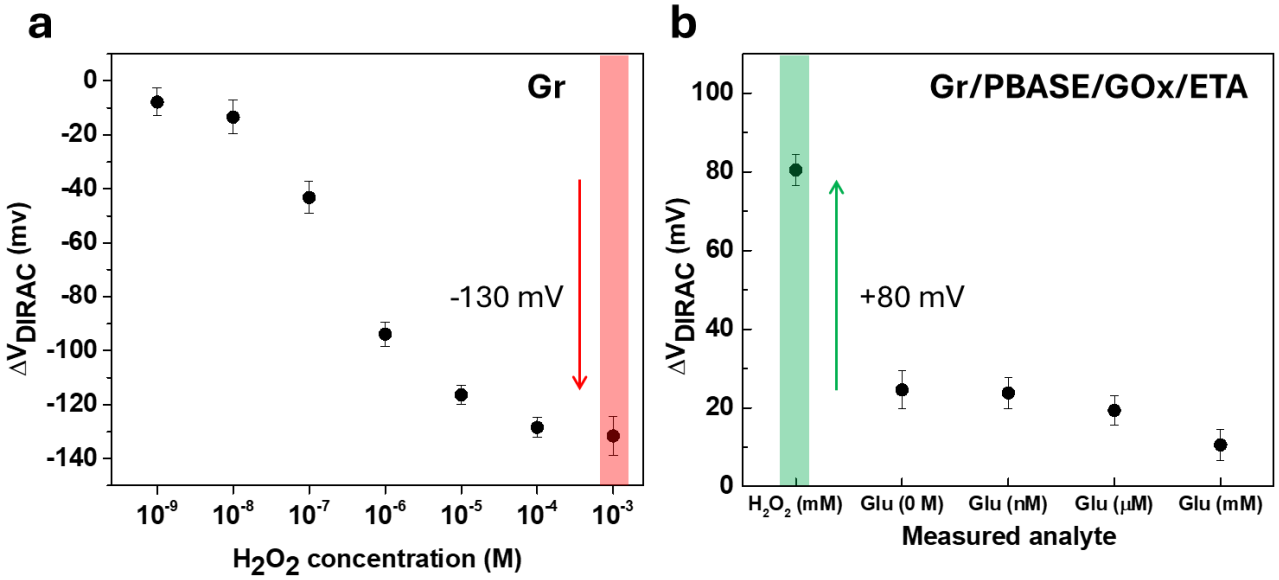

Figure S10. H_2O_2 measurements on EG-GFETs. (a) 1 nM-1mM H_2O_2 influence on V_{DIRAC} of bare graphene surfaces (only DDT passivation). The sensor shows n-type doping. (b) 1 mM H_2O_2 measured on Gr/PBASE/Gox/ETA, showing p-type doping. On the same sensor, after washing with 1 x PBS (Glu 0 M), glucose (Glu nM-Glu mM) was measured, with no variation of the V_{DIRAC} with increasing concentrations. The same concentration of H_2O_2 (1 mM) exhibited opposite behaviour for Gr and Gr/PBASE/GOx/ETA, confirming that glucose detection is based on the detection of H_2O_2.

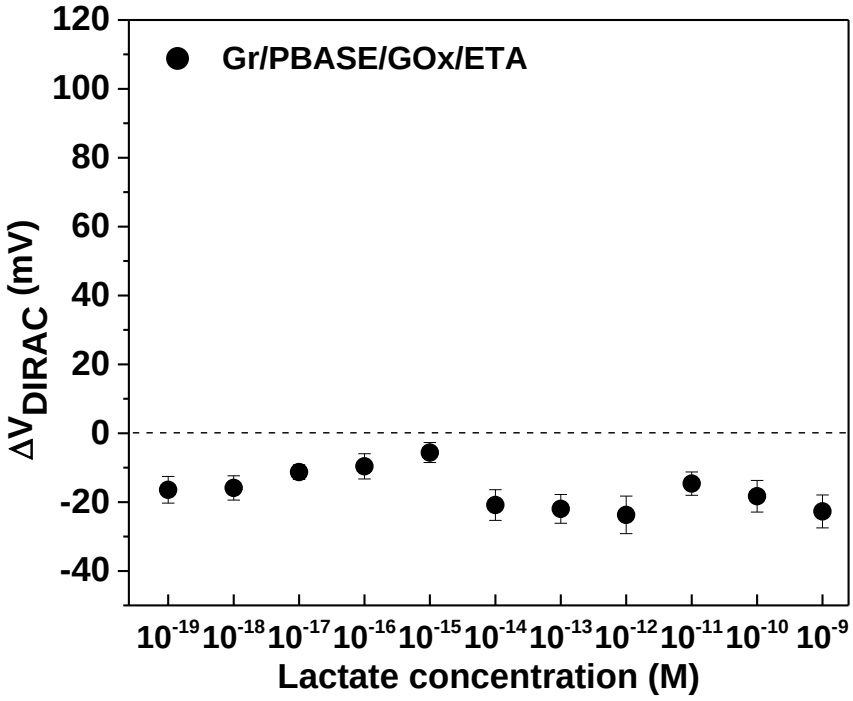

Figure S11. Calibration curve of lactate sensing on EG-GFETs in Gr/PBASE/GOx/ETA configuration within the same concentration range as glucose (aM-nM). As opposed to glucose, the sensor has an erratic behavior in response to lactate, proving the selectivity to glucose.

Table S1. Components used to fit the C 1 s spectra of the as-transferred graphene, Gr/PBASE, and Gr/PBASE/GOx samples. For each of them, the binding energy position in eV and the relative atomic concentration (at.%) are reported.

Sample	C-C Gr	p-p*	C-C	C-O/C-N	C=O	C=OO/N-C=O
Gr	284.5; 55.0%	290.9; 2.2%	284.9; 19.0%	286.1; 11.7%	287.1; 6.4%	288.8; 5.7%
Gr/PBASE	284.5; 56.7%	290.9; 2.3%	285.0; 18.2%	285.9; 14.6%	287.1; 4.1%	288.9; 3.1%
Gr/PBASE/GOx	284.5; 51.2%	290.9; 2.0%	285.0; 12.7%	285.9; 18.2%	287.2; 8.2%	288.5; 7.7%

Table S2. Relative at.% of carbon, nitrogen, and oxygen calculated from C 1 s, N 1 s, and O 1 s high-resolution peaks, respectively, for the as-transferred graphene, Gr/PBASE, and Gr/PBASE/GOx samples.

Sample	C tot.	N tot.	O tot.
Gr	64.9%	0.9%	34.2%
Gr/PBASE	68.1%	2.2%	29.7%
Gr/PBASE/GOx	67.1%	7.6%	25.3%

Table S1 shows the relative atomic percentage (at.%) of C, N, O for Gr, Gr/PBASE and Gr/PBASE/GOx samples. The C 1s fittings provide complementary information into the evolution of the C-O/C-N, C=O, and C=OO/N-C=O components (Table S2), which appear in all samples in addition to the two typical features of CVD graphene (*i.e.*, the main asymmetric peak at 284.5 eV and the corresponding shake-up satellite at 290.9 eV, and the C-C sp^3 component). In particular, the C-O/C-N component increases from 11.7 at.% to 18.2 at.% (from Gr to Gr/PBASE/GOx) owing to the high amount of amine and amide functional groups in the PBASE/GOx structure. This component slightly shifts toward lower binding energies (from 286.1 to 285.9 eV), indicating that several C–N bonds appear with respect to C–O bonds. For the sake of simplicity, we can assume that this component represents both C–O and C–N bonds, but they would be found at slightly different energies (286.3 and 285.9 eV, respectively). Therefore, if this peak moves to lower energy, the C-N contribution increases. Similarly, C=O (272.2 eV) and C=OO/N-C=O components increase, with a shift in the second component toward a lower binding energy (from 288.8 to 288.5 eV) due to the greater presence of amide groups, further confirming the effective biofunctionalization of the graphene surface.